Journal of Hydroscience and Hydraulic Engineering
Vol. 16, No. 1, May, 1998, 49-56

INFLUENCE OF SEASONAL METEOROLOGICAL VARIATIONS ON THERMAL ENERGY STORAGE IN SHALLOW AQUIFERS

By

Hiroshi Watanabe
Graduate Student, Department of Civil Engineering, Fukui University,
3-9-1, Bunkyo, Fukui, 910-8507, Japan

and

Teruyuki Fukuhara
Professor, Department of Civil Engineering, Fukui University,
3-9-1, Bunkyo, Fukui, 910-8507, Japan

and

Katsumi Adachi
1582-5, Kamikurata-cho, Totsuka-ku, Yokohama, Japan

SYNOPSIS

Aquifer Thermal Energy Storage (ATES) is the storage of local and seasonal thermal energy, such as natural summer heat, winter cold and industrial waste heat. An ATES enclosed by waterproof walls (Closed-Type ATES, CT-ATES) prevents the spread of water pollution caused by thermal, biological and chemical change. Using an ATES in a shallow aquifer has the advantage of low construction costs, reduction of heat transfer losses and easy maintenance. If the aquifer is shallow, however, the ATES may be sensitive to seasonal meteorological changes. This increases the uncertainties associated with the design and operation of seasonal thermal energy storage facilities.

This paper presents a numerical computation model that describes the characteristics of a CT-ATES in a shallow aquifer subjected to seasonal meteorological changes. The study showed that shallow CT-ATES could be effectively exploited but that it is necessary to carefully consider the effects of shallow seasonal temperature variations.

INTRODUCTION

Finding a positive usage of untapped energy can contribute to the reduction of CO_2 emissions into the atmosphere. Solar and wind energy is the most attractive natural energy resources, but their energy levels are sensitive to meteorological conditions and are therefore unreliable. Exploiting shallow terrestrial heat can contribute to finding a long-term solution for the energy crisis. While the energy density of terrestrial heat is relatively low, it is steady, and, in addition, regional differences of energy level are small compared with those associated with the high-level geothermal heat required for producing electric power. Aquifer thermal energy storage (ATES) includes the storage of local and seasonal thermal energy such as natural summer heat and winter cold as well as industrial waste heat [1), 2), 3)]. In general, there is a seasonal delay between demand and supply of natural energy. ATES systems can adjust the balance of energy supply and demand, and can encourage utilization of otherwise unreliable or low-level natural energy sources. Energy cost, efficiency and groundwater environmental considerations have become important for long-term, practical usage of thermal energy storage facilities.

The Closed-Type ATES (CT-ATES) introduced in this paper seems more applicable for preserving natural and social environments than the Opened-Type systems. In Closed-Type systems, a storage reservoir, extending down to an aquitard, is built in

an aquifer and surrounded with an impermeable vertical wall. Since the groundwater level in Japan is generally high, CT-ATES reservoirs can be built in shallow aquifers and this decreases cost while increasing construction safety. The disadvantage is, however, that CT-ATES systems using shallow aquifers may be susceptible to thermal interaction between the ground surface and the atmosphere because the heat insulation effect of the ground is relatively small.

The purpose of this paper is to describe the effect of seasonal meteorological changes on the energy storage properties of CT-ATES systems using a mathematical model proposed by the authors.

DERIVATION

Seasonal Thermal Energy Storage and Utilization of Natural Heat Energy

Figure 1 shows the seasonal relationship between supply and demand of natural heat energy. The upper and lower panels illustrate warm and cool energy storage, respectively. The curves show that a warm energy reservoir is charged during the summer and subsequently the warm energy is used in the following winter while a cool energy storage is charged during the winter and the energy is retrieved during the following summer. Since there is, in general, a seasonal lag between the demand and the available supply of energy, seasonal storage is needed in order to make the usage of natural energy as efficient as possible. Seasonal thermal energy storage can also contribute to minimizing the peak demand for power generation during summer time, as well as to the reduction of CO_2 emissions into the atmosphere.

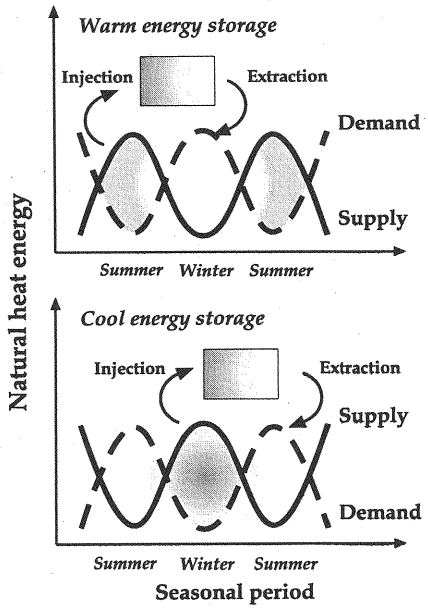

Figure 1 Seasonal relationship between supply and demand of natural heat energy

Aquifer Thermal Energy Storage

The injection and extraction of both cool and warm water, and the spatial configuration of the soil region involved, is shown in Figure 2 for three different types of ATES systems. Figure 2 (a) is a single-well type in a natural aquifer, Figure 2 (b) is a double-well type in a natural aquifer and Figure 2 (c) is a double-well type in a closed aquifer surrounded with impermeable walls. The configuration of Figure 2(c) is referred to as a Closed-Type ATES (CT-ATES) in this paper.

When open-type ATES systems have been in service for some time, groundwater contamination accompanying the injection and extraction of groundwater whose temperature deviates from the original groundwater temperature can have serious negative consequences. Activities of microorganisms can change the groundwater

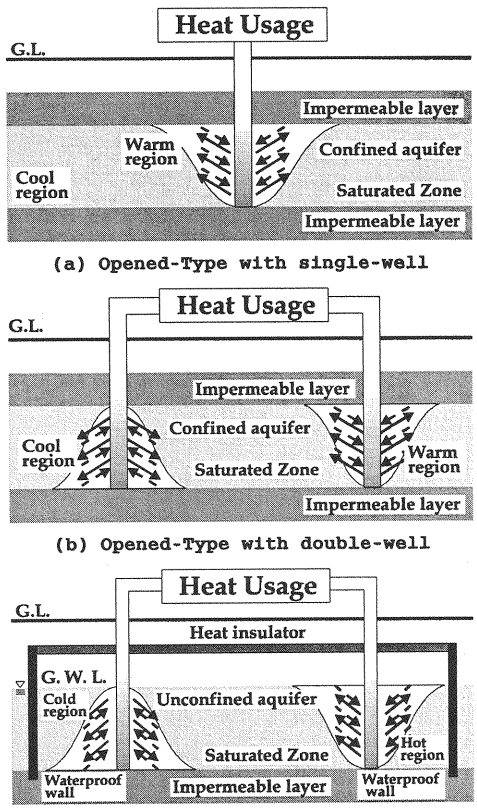

Figure 2 Type of ATES systems

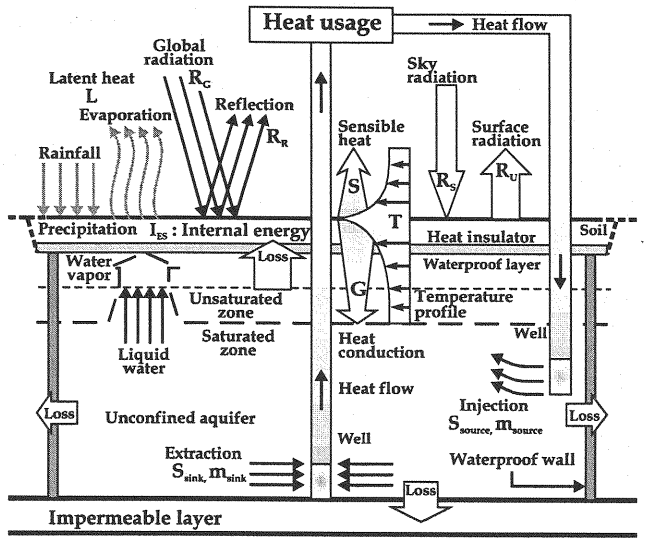

Figure 3 Schematic view of heat and moisture transfer between atmosphere and ground surface of the CT-ATES

Table 1 Parameters used in the numerical models

		Case-1	Case-2
D	(m)	1.5	10
H	(m)	10	10
H_∞	(m)	350	350
R	(m)	40	40
R_∞	(m)	320	320
k	(m^2)	3.2×10^{-11}	3.2×10^{-11}

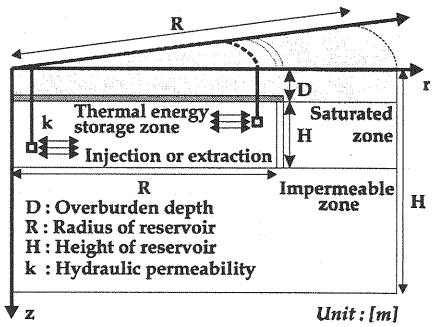

Figure 4 Numerical model of the CT-ATES

quality and can cause groundwater contamination. Such problems are avoided with Closed-Type systems.

Closed-Type ATES

Figure 3 indicates a schematic view of a double-well type CT-ATES in a shallow aquifer. A storage reservoir is built in an aquifer and enclosed by an impermeable wall to isolate it hydraulically from the surrounding aquifer. This is done to prevent contamination of the aquifer. Sometimes, a waterproof layer and /or a heat-insulating layer are also placed near the ground surface to reduce thermal effects caused by precipitation and surface temperature fluctuations.

In summer, cool water is extracted from the lower well and warm water is injected simultaneously to the upper well. In winter, these operations are reversed. Numerical computations for six annual cycles were found to be sufficient, to represent the long-term cyclic behavior of the reservoir.

In general, the groundwater table is high in Japan (in the range 1 to 10 m) and shallow aquifers are readily available. If it is possible to decrease the distance between the storage place and the location where the heat is needed transportation costs and heat losses can be reduced.

The ground surface temperature changes readily in response to varying meteorological conditions and these surface temperature changes propagate downward into the upper part of the shallow ATES reservoir.

Figure 3 also illustrates heat and moisture transfer in the ground surface layer. The main components of the surface heat budget are the net short wave solar radiation, the net long wave radiation, the sensible heat and the latent heat fluxes. The net sum of these components constitutes the heat available for conduction to or from the surrounding ground. The ground surface temperature depends on the balance of these heat fluxes.

Analysis of Heat and Mass Transfer in a Shallow CT-ATES [4]

The equations governing moisture transfer in the reservoir are:

$$-\nabla\cdot(\rho\,\vec{v}) + m_{source} - m_{sink} = 0 \qquad (1)$$

$$\vec{v} = -\frac{k}{\rho\nu}(\nabla P + \rho g\vec{\bar{z}}) \qquad (2)$$

where ρ is the density of water, $\vec{v}$ is the fluid velocity defined by Darcy's law, Eq. (2)., m_{source} and m_{sink} are the injection and extraction mass flux per unit volume and unit time, respectively, ∇ is the vector differential operator, k is the hydraulic permeability, ν is the kinetic viscosity, P is the pressure, $\vec{\bar{z}}$ is the unit vector of vertical direction and g is the acceleration of gravity. The density and viscosity terms in Darcy's law are given as functions depend on temperature (4). Isotropic permeability is assumed here. Compressibility effects are neglected and deformation of the porous media is not considered in Eq. (1).

Heat transfer within a closed storage reservoir is governed both by heat conduction and by advection associated with injection and extraction of thermal energy. The basic equation is written as:

$$(\rho c)\partial T/\partial t = \nabla(\lambda\nabla T) - (\rho c_w)\vec{v}\nabla T + S_{source} - S_{sink} \qquad (3)$$

where t is time, S_{source} and S_{sink} are the rate of injection and extraction of thermal energy per unit volume and unit time, respectively, (ρc_w) is the volumetric heat capacity of water, T is the temperature, (ρc) is the volumetric heat capacity of the aquifer and λ is the thermal conductivity.

The usual assumption, that the temperature at the upper boundary of the reservoir can be considered to be constant, is not appropriate because of the thermal interaction between the ground surface and the atmosphere.

The components of the energy balance at the ground surface are illustrated in Figure 3. The surface energy balance is described by:

$$\partial I_{ES}/\partial t = G + R_G + R_S - R_U - S - L \qquad (4)$$

where I_{ES} is the internal energy of the ground surface layer, R_S and R_U are the long wave radiation from the sky and the ground surface, respectively, R_G is the global incoming radiation from the sky, R_R is the radiation reflected upward from the ground surface, S is the sensible heat flux associated with air flow, L is the latent heat associated with evaporation and G is the ground heat flux by conduction. The effects of precipitation and latent heat can be safely ignored, provided that the ground surface is covered with an asphalt layer and the surface water is drained immediately.

Heat transfer in the ground surrounding the reservoir is assumed to be dominated by heat conduction.

Numerical Conditions

Figure 4 illustrates the numerical model used to simulate the seasonal heat exchange process in a CT-ATES and the notation used for the computations. H_∞ and R_∞ in Figure 4 are the dimensions in the axial and radial directions of the region simulated.

The parameter values assumed in the numerical model are presented in Table 1. Case-1 and Case-2 differ only in overburden depth. In Case-1, the overburden thickness is 1.5m while Case-2 is 10m.

The meteorological data used were taken from the daily reports of the Fukui Meteorological Observatory for the period April 1989 to April 1994. Composite data were created by averaging the values corresponding to the same date in each year. Annual patterns of the composite daily average, air temperature, air relative humidity, global radiation and wind velocity are shown in Figures 5 (a) and (b). These composite data were used for all annual cycles of the simulation.

Figure 6 illustrates the seasonal storage and the injection and extraction of cool or warm water. During the summer (July - September), the injected warm water is assumed to be at 35 °C. During the winter (January - March), the injected cool water

is assumed to be at 5 °C. The injection and extraction flow rates are both assumed to be 20 ℓ/min. [5].

Numerical Solutions and Discussions

Figures 7 (a) to (d) show computed isothermal contours (solid lines) within the reservoir and surrounding ground just after the sixth storage cycle. The broken lines indicate the closed reservoir boundary. The summer results (Figures 7 (a) and (c)) correspond to the time when the cool water usage has just been completed, i.e. the extraction of cool water is over. The warm water zone spreads horizontally from the strainer (■) of the upper well towards the center of the reservoir (r=0) along the top boundary (the ceiling of the CT-ATES reservoir) because of the buoyancy effect. Within the reservoir, there are few differences in the stratification and contour shape between Case-1 (thin overburden) and Case-2 (thick overburden). However, the minimum temperature in the reservoir occurs near the lower well, i.e. the final extraction temperature is 11 °C in Case-1 and 14 °C in Case-2.

On the other hand, the winter results, shown in Figures 7 (b) and (d) correspond to the time when the warm water usage has just been completed, i.e. the extraction of warm water is over. The cool zone grows near the central region of the reservoir and, at the same time, spreads horizontally from the center to the edge of the reservoir along the bottom boundary (the reservoir floor). Stratification in the reservoir develops more clearly in Case-2 than in Case-1 because the difference between maximum and minimum temperature is larger in Case-2. In addition, the maximum temperature in the reservoir that appeared near the upper well, i.e. the final extraction temperature in winter, is 18 °C in Case-1 and 22 °C in Case-2. This is caused by the difference in the overburden depth D, more precisely, the difference in the heat insulation effect of the overburden.

Figure 8 shows recovery rates of the cool and /or warm thermal energy storage. These are computed for each storage season (cool thermal energy storage in winter: January - March, warm thermal energy storage in summer: July - September). C_W is the recovery rate for the warm thermal energy during the following winter, C_C is the recovery rate for the cool thermal energy during the following summer and C_T is the total recovery rate. C_R is the ratio of the recovery rate in Case-1 to that in Case-2. The subscripts W and C represent warm and cool thermal energy, respectively. C_W, C_C, C_T and C_R are defined as follows;

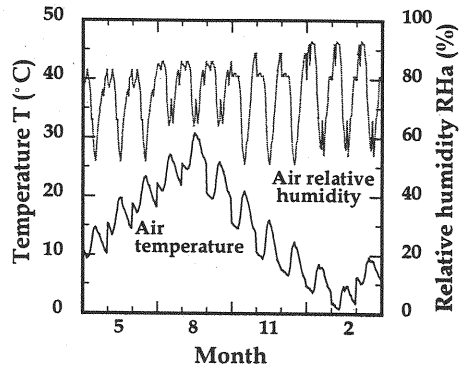

(a) Annual patterns of the air temperature T and air relative humidity RHa

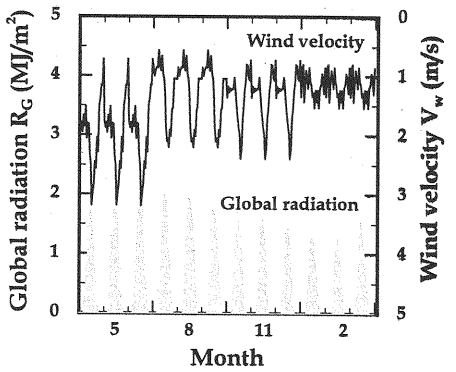

(b) Annual patterns of the global radiation R_G and wind velocity V_W

Figure 5 Annual patterns of the meteorological data in Fukui city

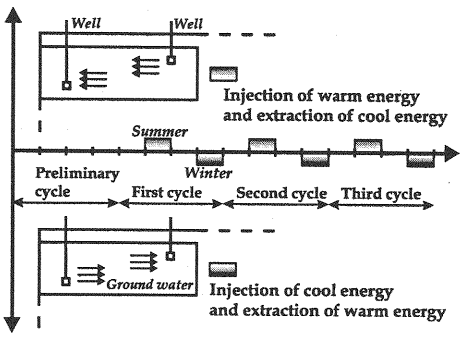

Figure 6 Seasonal storage and the injection and extraction of cool or warm water

$$C_W = E_W/I_W;\ C_C = E_C/I_C;\ C_R = C_1/C_2;\ C_T = \sum(E_W + E_C)/\sum(I_W + I_C) \qquad (5)$$

where E_W and E_C are the extracted warm and cool thermal energy, respectively, I_W and

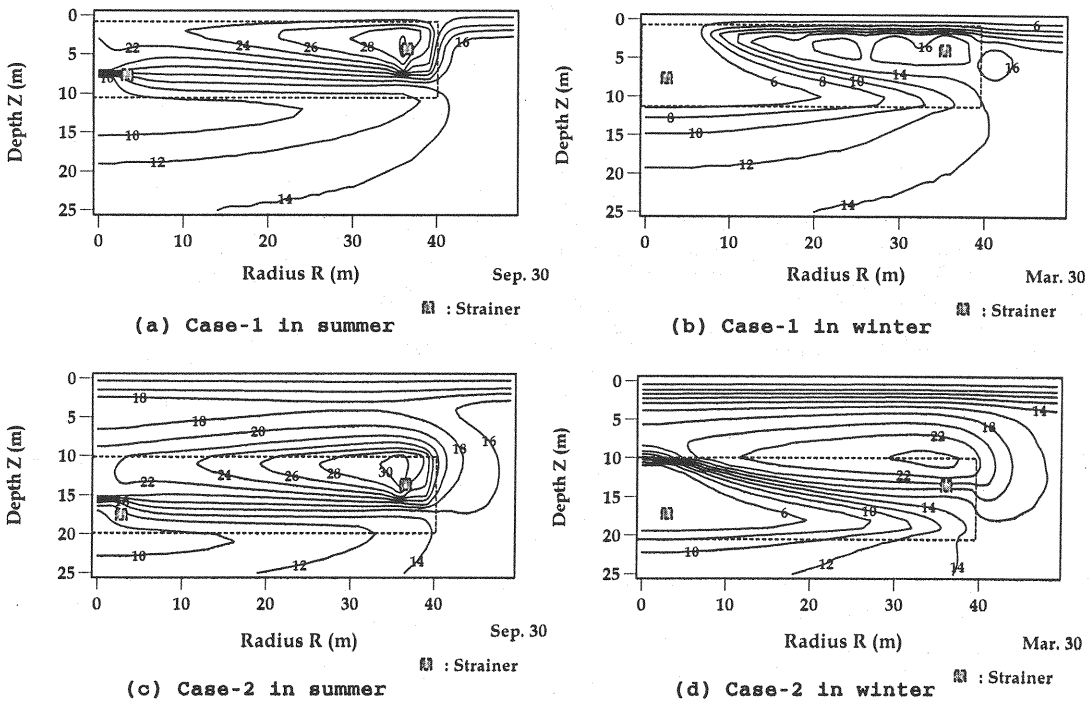

Figure 7 Isothermal contours within the reservoir and surrounding ground just after the sixth storage cycle

I_C are the injected warm and cool thermal energy, respectively, and the subscripts 1 and 2 denote Case-1 and Case-2, respectively. In Case-1, C_{W1}(○) gradually decreases but C_{C1}(△) gradually increases each year. In Case-2, C_{W2}(●) also gradually increases each year. C_{C2}(▲), however, decreases during the first two years but then becomes constant. Both C_T in Case-1, C_{T1} (---), and C_T in Case-2, C_{T2} (—), gradually increase with the elapsed years. C_{T2} is always higher than C_{T1} and the difference between C_{T1} and C_{T2} becomes large as the storage cycle increases. The C_R of warm thermal energy C_{RW}, symbol (□) is always less than one, and, although it decreases sharply at first later the rate of decrease diminishes. On the other hand, the C_R of cool thermal energy C_{RC}, symbol (▽), is always larger than one and increases from year to year.

From these observations, it is concluded that the shallow burial configuration of Case-1 is more efficient for a cool thermal energy storage while the deeper burial, Case-2, is more efficient for a warm thermal energy storage.

Knowledge of the time variations of heat fluxes across the walls of the reservoir is important for evaluating the characteristics of the recovery rates, and to optimize the selection of thermally effective materials for the containing walls. Figures 9(a) and (b) show the dimensionless heat flux, F_i/F_{2nd}, across the walls of the reservoir, where F_i is the (winter or summer) seasonal total heat flux across the ceiling and /or the floor during the i^{th} year. The subscript i corresponds to the year elapsed from initial start up. Values of the F_i/F_{2nd} ratio can be calculated only after the second year. All F_i/F_{2nd} continue to decrease, except Case-1 in summer (symbol (○)). Therefore, during summer, the warm thermal energy loss through the top boundary (ceiling) increases with the passing years. By comparing the summer F_i/F_{2nd} ratios, symbol (○) and (●) in Figure 9 (a), it can be concluded that the thin overburden allows the warm thermal energy stored in summer to be lost as time progresses. The behaviour of the heat flux across the lower boundary is illustrated in Figure 9(b). F_i/F_{2nd} in Case-2 (symbol (●)) varies from plus to minus with the elapsed year. This implies that, during summer, the heat energy initially flows upward from the ground across the bottom boundary (floor) to the reservoir and, then reverses direction because of the downward spread of the warm

water region caused by the injection of warm water from the upper well.

CONCLUSIONS

The energy storage properties of the Closed-Type seasonal thermal energy storage (CT-ATES) in a shallow aquifer were investigated. A numerical model developed by the authors was found to successfully describe the energy storage properties of a shallow CT-ATES. A configuration is susceptible to seasonal thermal interaction between the ground surface and the atmosphere.

The main conclusions can be summarized as follows;

1) the effect of the seasonal thermal interaction between the ground surface and the atmosphere on the performance of the CT-ATES can not be ignored,
2) the final extraction temperature of warm water is higher in the CT-ATES reservoir with a thick overburden than in that with a thin overburden, however, the opposite is true for the final extraction temperature of cool water, it is cooler with a thin overburden,
3) the CT-ATES with a thin overburden is more efficient for providing cool thermal energy storage in summer than for warm thermal energy storage in winter.

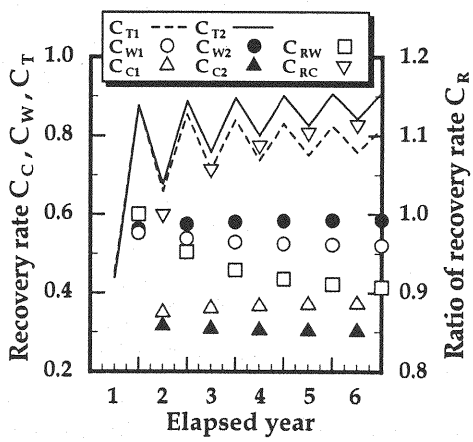

Figure 8 Time series of coefficients of warm and cool thermal energy recovery

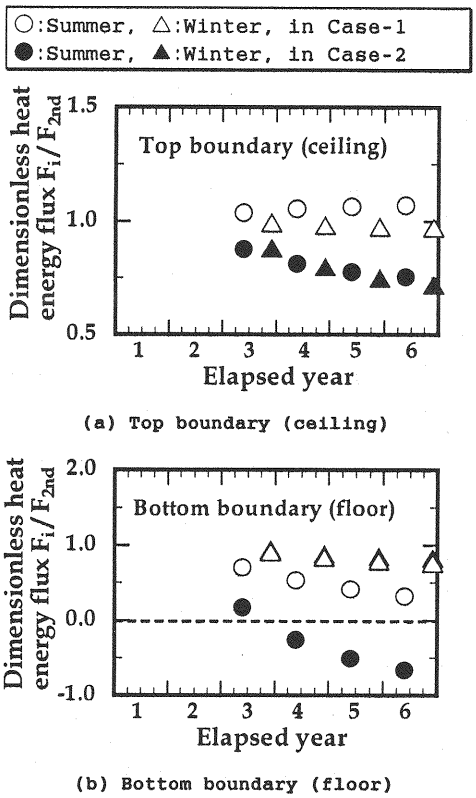

Figure 9 Time series of dimensionless heat energy flux across boundary of the CT-ATES

REFERENCES

1) Lejeune, J. M.: Stockage de Chaleur en Nappe de Surface-Les Pilotes de Montreuil de Lyon-Gerland, Houille Blanche No. 3/4, pp. 319-324, 1985.
2) Hahne, E. and Hornberger M. F.: Combined heat and cool storage in a gravel/water pit, Proceedings of 6th International Conference on Thermal Energy Storage, CALORSTOCK ' 4, Espoo, Finland, pp. 365-372, 1994.
3) Adachi, K., Fukuhara T. and Watanabe H.: Thermal flow problems to be solved in aquifer thermal energy storage, Proceedings of Japan Association of Groundwater Hydrology, Kyoto, Japan, pp. 128-133, 1995.
4) Kangas, M. T. and Lund P. D.: Thermal analysis of aquifer energy storage system, Helsinki University of Technology, Report TKK-F-A623, Espoo, Finland, 1988.
5) Moriyama, K., Hayashi T., Fukuhara T., Watanabe H. and Adachi K.: Applying terrestrial heat and control of pavement temperature using Bore-hole Heat Exchange System, Proceedings of Japan Association of Groundwater Hydrology, Kyoto, Japan, pp. 142-145, 1995.

APPENDIX - NOTATION

The following symbols are used in this paper:

C_C	-	= recovery rate for the cool thermal energy;
C_{C1}	-	= C_C in Case-1 (with thin overburden);
C_{C2}	-	= C_C in Case-2 (with thick overburden);
C_R	-	= ratio of the recovery rate in Case-1 to that in Case-2;
C_{RC}	-	= C_R of cool thermal energy;
C_{RW}	-	= C_R of warm thermal energy;
C_T	-	= total recovery rate;
C_{T1}	-	= C_T in Case-1 (with thin overburden);
C_{T2}	-	= C_T in Case-2 (with thick overburden);
C_W	-	= recovery rate for the warm thermal energy;
C_{W1}	-	= C_W in Case-1 (with thin overburden);
C_{W2}	-	= C_W in Case-2 (with thick overburden);
D	m	= overburden depth;
E_C	kJ/m^3h	= extracted cool thermal energy;
E_W	kJ/m^3h	= extracted warm thermal energy;
F_1/F_{2nd}	-	= dimensionless heat flux across the walls of the reservoir;
g	m/s^2	= acceleration of gravity;
G	W/m^2	= ground heat flux by conduction;
H	m	= height of reservoir;
H_∞	m	= height of numerical region;
I_C	kJ/m^3h	= injected cool thermal energy;
I_{ES}	kJ/m^3	= internal energy of the ground surface layer;
I_W	kJ/m^3h	= injected warm thermal energy;
k	m^2	= hydraulic permeability;
L	w/m^2	= latent heat associated with evaporation;
m_{source}	kg/m^3h	= mass flux of injection per unit volume and unit time;
m_{sink}	kg/m^3h	= mass flux of extraction per unit volume and unit time;
P	Pa	= pressure;
r	-	= coordinate in radial direction;
R	m	= radius of reservoir;
R_G	MJ/m^2	= global incoming radiation from the sky;
R_R	MJ/m^2	= radiation reflected upward from the ground surface;
R_S	W/m^2	= long wave radiation from the sky;
R_U	W/m^2	= long wave radiation from the ground surface;
R_∞	M	= radius of numerical region;
S	w/m^2	= sensible heat flux associated with air flow;
S_{source}	kJ/m^3h	= injection thermal energy density per unit volume and unit time;
S_{sink}	kJ/m^3h	= extraction thermal energy density per unit volume and unit time;
t	H	= time;
T	K	= temperature;
$\vec{v}$	m/h	= fluid velocity defined by Darcy's law;
z	-	= coordinate in vertical direction;
$\vec{\bar{z}}$	-	= unit vector of vertical direction;
λ	W/mK	= thermal conductivity;
ν	m^2/s	= kinetic viscosity;
ρ	kg/m^3	= density of water;
ρc_w	kJ/m^3K	= volumetric heat capacity of water;
ρc	kJ/m^3K	= volumetric heat capacity of the aquifer; and
∇	-	= vector differential operator.

(Received December 2, 1997; revised February 5, 1998)